2012-5-25

Investigation of Interfacial Oxidation Control Using Sacrificial Metallic Al and La Passivation Layers on InGaAs

Barry Brennan, *et al.*

JVSTB
JOURNAL OF VACUUM SCIENCE AND TECHNOLOGY B

Investigation of interfacial oxidation control using sacrificial metallic Al and La passivation layers on InGaAs

Barry Brennan, Marko Milojevic, Roccio Contreras-Guerrero, Hyun-Chul Kim, Maximo Lopez-Lopez et al.

Citation: J. Vac. Sci. Technol. B **30**, 04E104 (2012); doi: 10.1116/1.4721276
View online: http://dx.doi.org/10.1116/1.4721276
View Table of Contents: http://avspublications.org/resource/1/JVTBD9/v30/i4
Published by the AVS: Science & Technology of Materials, Interfaces, and Processing

Investigation of interfacial oxidation control using sacrificial metallic Al and La passivation layers on InGaAs

Barry Brennan[a] and Marko Milojevic
Department of Materials Science and Engineering, University of Texas at Dallas, Richardson, Texas 75080

Roccio Contreras-Guerrero
Department of Physics, CINVESTAV-IPN, Apartado Postal 14-740, México D.F. 07000, Mexico

Hyun-Chul Kim
Department of Materials Science and Engineering, University of Texas at Dallas, Richardson, Texas 75080

Maximo Lopez-Lopez
Department of Physics, CINVESTAV-IPN, Apartado Postal 14-740, México D.F. 07000, Mexico

Jiyoung Kim and Robert M. Wallace[b]
Department of Materials Science and Engineering, University of Texas at Dallas, Richardson, Texas 75080

(Received 16 February 2012; accepted 5 May 2012; published 25 May 2012)

The ability of metallic Al and La interlayers to control the oxidation of InGaAs substrates is examined by monochromatic x-ray photoelectron spectroscopy (XPS) and compared to the interfacial chemistry of atomic layer deposition (ALD) of Al_2O_3 directly on InGaAs surfaces. Al and La layers were deposited by electron-beam and effusion cell evaporators, respectively, on $In_{0.53}Ga_{0.47}As$ samples with and without native oxides present. It was found that both metals are extremely efficient at scavenging oxygen from III–V native oxides, which are removed below XPS detection limits prior to ALD growth. However, metallic Ga/In/As species are simultaneously observed to form at the semiconductor–metal interface. Upon introduction of the samples to the ALD chamber, these metal bonds are seen to oxidize, leading to Ga/In–O bond growth that cannot be controlled by subsequent trimethyl-aluminum (TMA) exposures. Deposition on an oxide-free InGaAs surface results in both La and Al atoms displacing group III atoms near the surface of the semiconductor. The displaced substrate atoms tend to partially oxidize and leave both metallic and III–V oxide species trapped below the interlayers where they cannot be "cleaned-up" by TMA. For both Al and La layers the level of Ga–O bonding detected at the interface appears larger then that seen following ALD directly on a clean surface. [http://dx.doi.org/10.1116/1.4721276]

I. INTRODUCTION

Research on III–V substrates for the microelectronics industry has defined the quality of the insulator/substrate interface as arguably the greatest obstacle for widespread adaptation of this material system in future technology nodes.[1] Without the use of an interface passivation layer (IPL), the defect density of this interface is such that the Fermi level becomes pinned and an anomalous frequency dispersion phenomenon in accumulation capacitance is observed.[2] Recent work has revisited the use of thin IPLs for III–V metal-oxide-semiconductor (MOS) gate stacks with great success. Work by Oktyabrsky *et al.*[3] and Zhu *et al.*[4] has shown that parameters such as oxide and IPL thickness can be varied in order to optimize the performance of MOS capacitors utilizing Si-IPLs. The general hypothesis is that these layers inhibit the formation of surface oxides of Ga and As during device processing, which likely result in the formation of the defects leading to Fermi level pinning. For example, a recent study by Hinkle *et al.*[5] demonstrated that the deleterious capacitance behavior is related to the formation of interfacial Ga_2O_3. Additionally it was shown that the Ga^{1+} oxidation state of gallium (Ga_2O) does not appear to contribute to frequency dispersion. Unfortunately the use of an Si-IPL leads to the formation of a thin, relatively low-*k* SiO_2 layer, which would put a limit on the attainable gate stack capacitance of devices based on this technology. With this in mind, the work presented here attempts to evaluate the use of metallic Al- and La-IPLs that, when oxidized, form high-*k* oxides. This study is performed *in situ*, where with the use of monochromatic x-ray photoelectron spectroscopy (XPS), the obtained interfaces are evaluated for their overall chemical composition and behavior during subsequent atomic layer depositions (ALD) using an *in situ* "half-cycle" approach outlined in previous studies.[6–8] The impact of the metallic layers, on both oxidized and oxide-free $In_{0.53}Ga_{0.47}As$ surfaces, is compared to the "clean-up effect" by trimethyl-aluminum (TMA) during ALD.[8,9]

The formation of metal–GaAs interfaces has been extensively researched in terms of the generation of Ohmic contacts and Schottky barriers at the metal semiconductor interface, with Al, Cu, Ni, Ag, Ge, and Si getting particular attention.[10–13] In the case of deposition of Al on GaAs, Al is seen to replace Ga (and for InGaAs the same is likely to be the case for the In also) in the subsurface layers forming AlAs,[11] liberating the Ga and In to form metal states through the replacement reaction,

[a]Electronic mail: barry.brennan@utdallas.edu
[b]Electronic mail: rmwallace@utdallas.edu

$$xAl + (In)GaAs \rightarrow (In)Ga_{1-x}Al_xAs + x(In)Ga, \quad (1)$$

as well as the interaction with any excess As that forms during deposition through the following reaction:

$$Al + (In)GaAs_{1+y} \rightarrow AlAs_{\Delta} + (In)GaAs_{1+(y-\Delta)}. \quad (2)$$

Second layer Ga sites are thermodynamically more favorable than top layer sites,[12] and smaller net kinetic energy barriers than third and deeper layers. These interactions are metal dependent, and in the case of Au deposition, the Au is seen to interact preferentially with Ga, generating excess As.[13]

What is not clear, however, is what happens upon subsequent oxidation of these layers and whether it is possible to remove the defects that are generated during the deposition process, and to what extent this process compares to when a thin native oxide layer is already present at the interface. If we assume that the IPL will scavenge any oxygen present at the interface (or present during exposure to further deposition processes),[14] in the case of Al this will likely form Al_2O_3 at the interface. While Al_2O_3 has a higher k value than that of SiO_2, it will still be desirable to have a material with larger k value present at the interface. For this reason, lanthanum oxide has been proposed as a potential high-k material for integration into next generation semiconductor devices. However, unlike Al, the interaction between La metal and the (In)GaAs surface is not well known, with very little information available regarding the interfacial chemistry that takes place upon deposition. This is likely due to the very high reactivity of La, which necessitates the use of *in situ* deposition and characterization techniques.[15]

The effect of metal deposition and subsequent ALD of Al_2O_3 is first compared to direct ALD Al_2O_3 on an oxide-free surface. Considering the first cycle of the ALD process involves the interaction of the TMA molecule with the InGaAs surface, this allows for a direct comparison between the effect of substrate–metal ion interactions and Al growth through interactions between the semiconductor surface (metal dep) and the metal ligands (ALD). Since ALD is a surface controlled deposition process,[16] interactions between the Al in the TMA and subsurface layers of the InGaAs substrate are unlikely to take place, reducing the potential for metallic Ga and In generation. The growth of Al on the surface is limited by the number of ligand interactions that take place; until the surface is saturated by TMA reaction products. Since the Al is chemisorbed at the surface it is also unlikely to propagate into the substrate, with any excess energy generated in the interaction transferring to the liberated reaction products. However, based on the previously reported clean-up effect,[7] the possibility of improving the interface between the substrate and the oxide layer after IPL deposition presents a potential method for enhancing the effectiveness of the IPL layer.

II. EXPERIMENT

Metallic Al- and La-IPLs were deposited *in situ* from electron-beam and effusion sources, respectively, to a thickness of 1 nm, measured with a quartz crystal monitor. The behavior of the Al- and La-IPLs was explored on oxide-free $In_{0.53}Ga_{0.47}As$ surfaces as well as on a sample that underwent a 3 min etch in NH_4OH to remove the native oxide that was present due to atmospheric exposure.

The $In_{0.53}Ga_{0.47}As$ used in this study was grown lattice matched on InP obtained from Intelliepi.[17] The oxide-free surface is obtained from wafers that were initially protected by a 50 nm thick arsenic capping layer deposited following MBE growth of the $In_{0.53}Ga_{0.47}As$ layer.[18] This film prevents native oxides from forming during *ex situ* handling but can then be desorbed in ultrahigh vacuum (UHV) with a 30 min anneal at 430 °C. In order to study the ability of the metal IPLs to modify native oxides some samples were obtained without this As cap. They were initially degreased for 1 min in each of acetone, methanol, and isopropyl alcohol. The native oxides were partially removed using an NH_4OH dip for 3 min followed by a rinse in flowing de-ionized water for <10 s. Samples were then mounted and introduced into a UHV system in less than 10 min. A dual chamber ALD reactor[19] integrated to a UHV multitechnique deposition/characterization system was used for this *in situ* study.[20] TMA was used as the Al precursor for subsequent Al_2O_3 formation using a water deposition chemistry at 300 °C.

XPS was carried out using a monochromatic Al $K\alpha$ x-ray source ($h\nu = 1486.7$ eV) with a linewidth of 0.25 eV, and a 125 mm seven channel hemispherical electron energy analyzer at a pass energy of 15 eV. This is contained in a dedicated analysis chamber maintained at a base pressure of $<5 \times 10^{-11}$ mbar and connected through a UHV transfer tube to the *in situ* deposition chambers.[21] XPS spectra were taken of the As 3*d*, As $2p_{3/2}$, Ga 3*d*/In 4*d*, Ga $2p_{3/2}$, In $3d_{5/2}$, O 1*s*, C 1*s*, Al 2*p*, La 3*d*, and La 4*d* core levels to ensure consistent information was attained from different core levels of the same element, where possible. XPS peak fitting was carried out using AANALYZER,[22] with details of the peak fitting process described previously.[23,24]

III. RESULTS AND DISCUSSION

A. Al deposition

Figure 1 shows the highly surface sensitive[25] Ga $2p_{3/2}$, As $2p_{3/2}$, as well as the In $3d_{5/2}$ spectra from the oxide-free InGaAs sample. The indium region, due to the lower (higher) binding (kinetic) energy of the core level, is not as surface sensitive as either that of the gallium or the arsenic 2*p* spectra shown here; however, it is the most surface sensitive core level available using an Al $K\alpha$ x-ray source. The In spectra are further complicated due to the asymmetric nature of the In 3*d* core level line shape, which broadens the spectra at the higher binding energy side of the peak. This can lead to complications in spectral interpretation as this is a region in which indium oxidation states would be expected to appear. In order to simulate this asymmetric peak line shape, an extra peak is linked to the In 3*d* peak when it is clear that there is no detectable indium oxide present, based on the O 1*s* core level spectra. This line shape is then maintained throughout the analysis unless it is clear that the natural line shape of the core level has changed and cannot be fitted

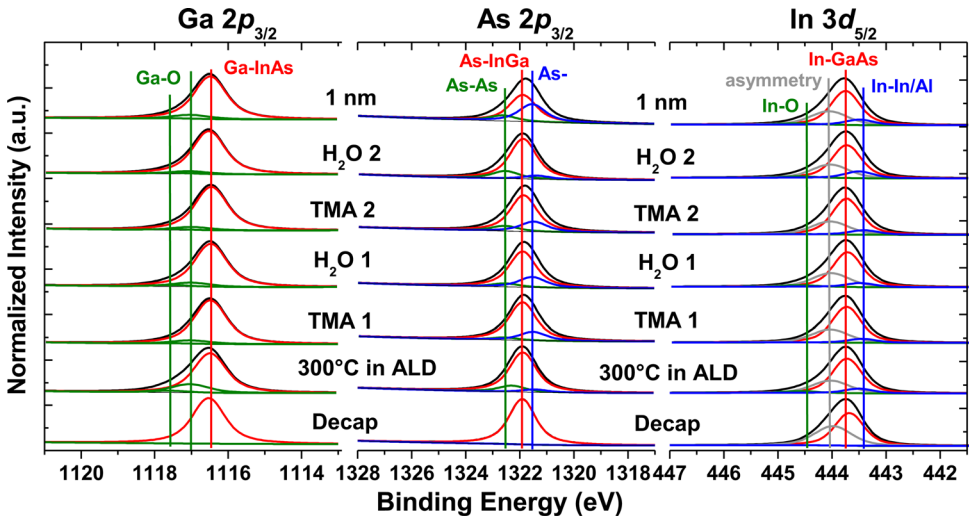

FIG. 1. (Color online) Ga $2p_{3/2}$, As $2p_{3/2}$, and In $3d_{5/2}$ core level spectra from a decapped InGaAs sample, following exposure to the ALD reactor chamber, and then after subsequent half-cycle ALD precursor exposures up to 1 nm of Al_2O_3. An extra feature is introduced in the In spectra to fit the asymmetry of the In line shape. See the text.

accurately without changing the parameters of the extra component. Due to the thermodynamic stabilities of indium related compounds[26] it is expected that their behavior mimics gallium closely and this is further monitored and cross referenced to ensure as accurate peak deconvolution as possible. Following desorption of the As capping layer, the surface shows evidence of only Ga–As–In bonds, and from Fig. 2 the O 1*s* core level signal is below the level of detection and is referred to herein as an "oxide-free" surface.

Prior to the first TMA exposure the sample is inserted into the ALD reactor for 30 min in order to determine the effect of temperature and any residual species in this chamber. This exposure to the ALD reactor at 300 °C maintained at ~9 mbar results in mainly Ga^{1+} formation and minimal Ga^{3+} states appearing in the Ga 2*p* spectra,[5] located at 0.55 and 1.1 eV from the bulk peak, respectively. Simultaneously, a signal in the O 1*s* spectra is detected (Fig. 2). Additionally As–As bonding is detected upon reactor exposure and is expected to accompany any Ga–O bond formation due to breaking of Ga–As bonds. As shown previously,[7,8] the first TMA pulse reduces Ga^{3+} bonds below the level of detection while some Ga^{1+} remains. This transfer of oxygen from the substrate oxides is illustrated in the O 1*s* region in Fig. 2 as the peak shifts to a higher binding energy, with the emergence of a peak component associated with Al–O formation (~531.2 eV). The As–As peak is also reduced, with the concurrent emergence of a lower binding energy "As^-" peak, suggesting possible formation of As surface states (dangling bonds or dimers), or As–Al bonds. The interface appears chemically passivated as, following further TMA and water exposures, the chemical configuration of gallium atoms is not significantly affected. This behavior is reflected in the ratio of the fitted oxide peak components to the bulk peak area shown in Fig. 3.

Interestingly, the As–As bond concentration relative to the bulk As–Ga bond appears to increase as the Al_2O_3 film grows. A possible explanation for this behavior is offered by Huang *et al.*,[27] as they observed arsenic at the top of their

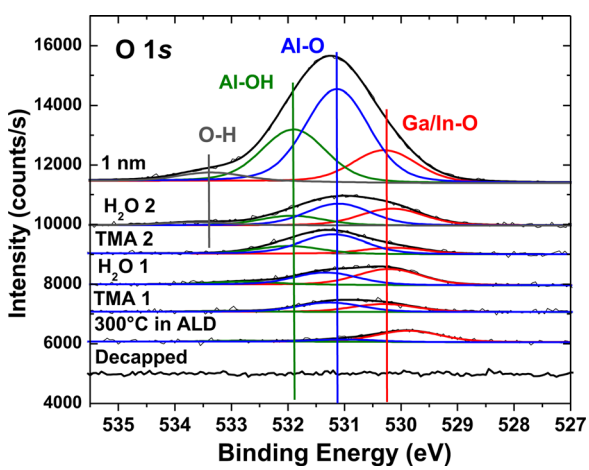

FIG. 2. (Color online) O 1*s* core level spectra from a decapped InGaAs sample following exposure to the ALD reactor chamber, and then after subsequent half-cycle ALD precursor exposures up to 1 nm of Al_2O_3.

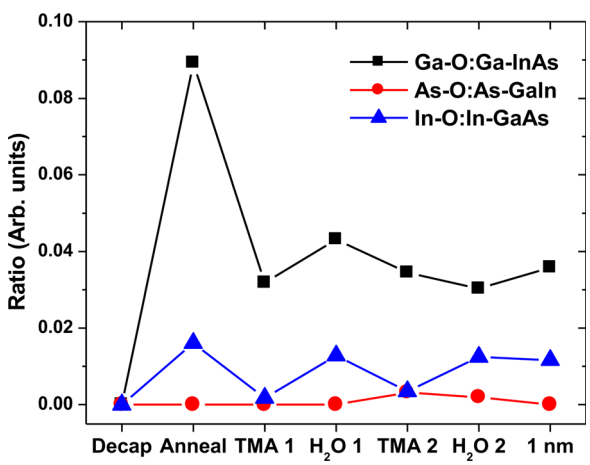

FIG. 3. (Color online) Ratio of the fitted core level oxide to bulk peak components from the Ga $2p_{3/2}$, As $2p_{3/2}$, and In $3d_{5/2}$ spectra.

ALD films. Incorporation of As–As into the dielectric or its segregation at the top of the grown layer would result in less photoelectron attenuation relative to the signal coming from the bulk As–Ga substrate atoms. This type of behavior would manifest itself as the increase of As–As/As–Ga ratio with film thickness that is observed in this study. Due to the utilization of highly surface sensitive As 2*p* spectra this effect would be detectable even at very small (<1 nm) Al_2O_3 thicknesses.[25] Alternatively, the oxidation of the surface has been shown to result in As–As bonding at the interface according to some recent first-principles models.[28–30] By peak fitting the As 2*p* and the As 3*d* core level peaks, taking into account the relative sensitivity factors for the photoemitted electrons, and monitoring the ratio of the fitted area of the As–As to the bulk peaks, the ratio is seen to be very similar for both core levels upon Al_2O_3 deposition. This suggests that the As–As is located at the interface, as the increased surface sensitivity of the As 2*p* peak would create a divergence in the ratio if the As–As was located at the surface.

Figure 4 shows the Ga $2p_{3/2}$, As $2p_{3/2}$, and In $3d_{5/2}$ spectra from a decapped $In_{0.53}Ga_{0.47}As$ surface as it undergoes metal Al-IPL deposition and subsequent growth of 1 nm ALD Al_2O_3. Following the deposition of 1 nm of Al metal, the formation of a metallic Ga chemical state is detected at a binding energy of ~0.9 eV below that of the bulk peak. It is unclear if these are Ga–Ga or Ga–Al bonds since, due to their similar electronegativities,[31] both peaks are expected to appear at very similar binding energies. Similarly, the In 3*d* spectra also show the emergence of a lower binding energy peak indicating In–Al bonding taking place, at an elevated level compared to that of Ga, suggesting In has a greater affinity for bonding to Al. These chemical changes are further accompanied by a broadening of the As $2p_{3/2}$ spectra due to the emergence of a peak at ~0.7 eV lower binding energy, indicating As–Al formation, although at lower levels than seen in either the In or Ga spectra. The formation of Al–substrate bonds is also visible in the Al 2*p* region shown in Fig. 5(a). Overall these observations are a symptom of a chemical disruption of the pristine III–V surface through interaction of the metal atoms with the substrate, which was not the case with the first ALD cycle, highlighting that the presence of ligand interactions during the ALD process results in very different behavior compared to that for the metal atom only.

Exposure to the ALD chamber ambient causes some Ga^{3+}, Ga^{1+}, and In oxidation states to appear and simultaneously the metallic Ga and In peaks to be diminished. As evident from Fig. 5(a), the Al-IPL is almost fully oxidized at this stage, likely causing the oxidation of the Ga and In at the interface with the substrate. These oxide states appear to be located below the Al-IPL as further exposures to TMA and water pulses do not produce large changes in the spectrum, as evidenced by the ratio of the oxides to the substrate peaks in Fig. 5(b). Unfortunately, as shown by Hinkle *et al.*,[5] the presence of Ga^{3+} chemical states at the interface will likely result in undesirable electrical characteristics.

The ability of TMA to clean-up interfacial oxides is largely due to the inherently higher affinity for oxygen exhibited by Al as compared to Ga and As.[32] This property is explored by depositing metallic Al on the InGaAs surface that was treated with NH_4OH. The Ga $2p_{3/2}$/As $2p_{3/2}$/In $3d_{5/2}$ spectra in Fig. 6 show residual gallium and arsenic oxides as well as As–As commonly found following an NH_4OH treatment.[33] Remarkably, following the deposition of the Al-IPL, both As and Ga oxides are reduced below the level of detection of XPS while As–As bonding is also diminished. As discussed earlier, the O 1*s* peak following the TMA exposure represents a mixture of residual substrate oxides and the newly formed Al–O bonds at higher binding energy. However, following the deposition of the Al-IPL the O 1*s* peak in Fig. 7(a) shifts dramatically to the O–Al position. This is consistent with the complete reduction of substrate oxides seen in Fig. 6.

As per previous ALD studies, this again suggests that the clean-up effect, as a result of interaction of the native oxides with TMA, proceeds through a ligand exchange mechanism,

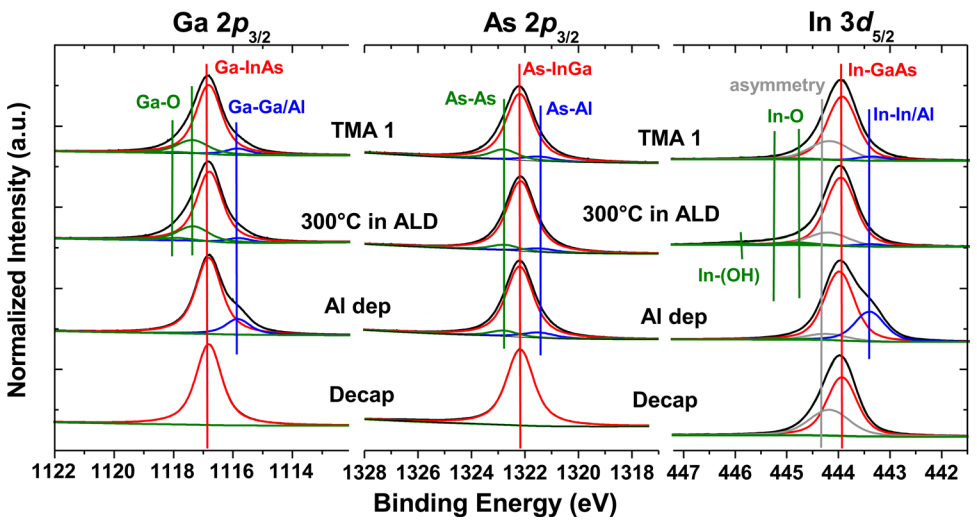

FIG. 4. (Color online) Ga $2p_{3/2}$, As $2p_{3/2}$, and In $3d_{5/2}$ core level spectra from a decapped InGaAs sample and following subsequent 1 nm deposition of Al metal and half-cycle ALD of 1 nm of Al_2O_3.

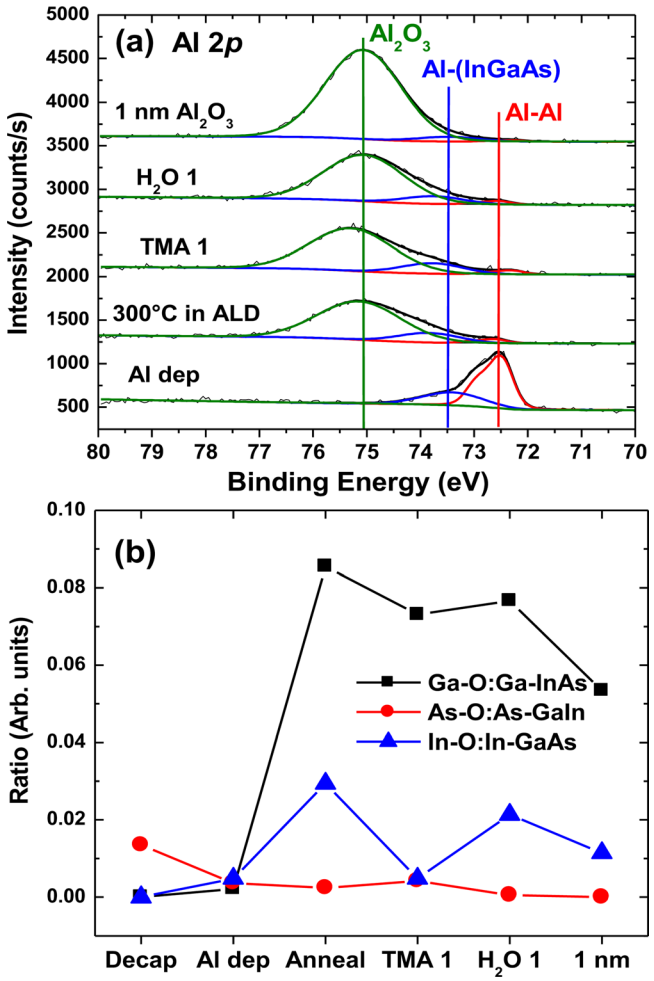

FIG. 5. (a). (Color online) Al 2*p* core level spectra from a decapped InGaAs sample and following subsequent 1 nm deposition of Al metal and half-cycle ALD of 1 nm of Al_2O_3 and (b) the ratio of the fitted oxide to bulk peak components from the Ga $2p_{3/2}$, As $2p_{3/2}$, and In $3d_{5/2}$ spectra.

whereby the valency of the dominant oxide for the incoming metal precursor dictates which native oxide states will be removed.[34,35] The removal of the native oxides upon the deposition of metallic Al is not restricted to relying on surface chemical interactions through ligand exchanges to allow interaction with the oxide, and as such is likely to be solely dependent on the magnitude of the formation energies for the individual states. The Gibbs free energy for Al_2O_3 is reported to be significantly lower than that of any of the native oxide states present on the InGaAs surface and as such would be the most energetically favorable system.[1,32]

Another significant difference to the TMA clean-up effect is that these Al-IPL experiments produce a detectable reduction product of the native oxides; metalliclike states. Therefore, in the presence of a native oxide on the surface the Al-IPL will reduce these rather than attacking the substrate as follows:

$$(\mathrm{Ga/In/As})_2\mathrm{O}_3 + 2\mathrm{Al} \rightarrow \mathrm{Al}_2\mathrm{O}_3 + 2(\mathrm{Ga/In/As}). \quad (3)$$

This is contrary to the clean-up with TMA on the III–V surface, which produces no detectable reduction products and cannot completely remove Ga–O bonding. This further suggests that the species produced by TMA interactions are indeed volatile, as proposed elsewhere.[7–9] Despite its inability to fully reduce native oxide bonds, and specifically Ga_2O, with the trivalent TMA molecule mostly targeting the trivalent oxide states through a ligand exchange mechanism, the volatilization of the reduced gallium species is likely critical to the abrupt interfaces produced with ALD on III–V surfaces.[36]

The suggestion is then that Al-IPL is indeed a poor chemical passivant, as highly reactive metallic species are left at the interface that immediately oxidizes inside the ALD reactor, although some Al–substrate bonds are seen to persist throughout, as indicated by the Al 2*p* spectra in Fig. 7(b). Looking at the ratio of the oxide components to the substrate peaks in Fig. 7(c) indicates that the level of Ga–O bonding does not change as a result of exposure of the sample to TMA, whereas the As and In–O ratios are seen to decrease to within detection limits with successive cycles. This suggests that the Ga–O persists at the interface between the Al–O and the substrate, preventing oxide clean-up from taking place.

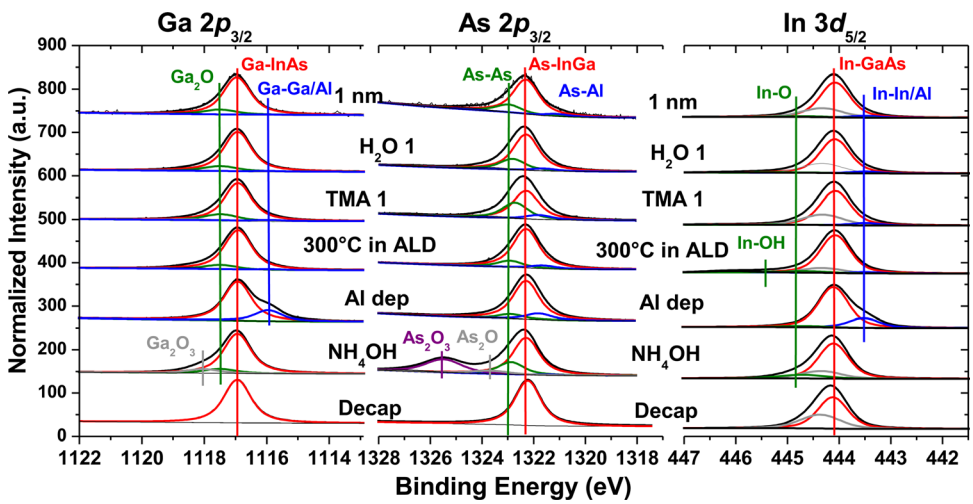

FIG. 6. (Color online) Ga $2p_{3/2}$, As $2p_{3/2}$, and In $3d_{5/2}$ core level spectra from a decapped InGaAs sample and after subsequent *ex situ* NH_4OH treatment, 1 nm of Al deposition half-cycle up to 1 nm of ALD Al_2O_3.

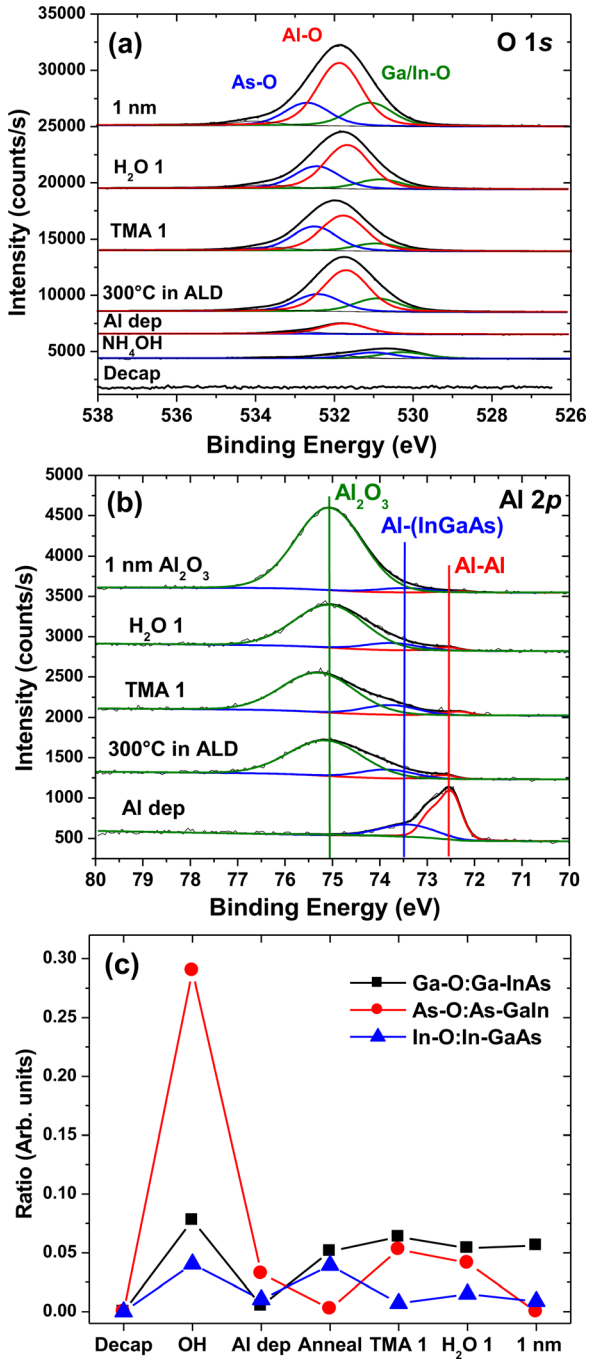

FIG. 7. (a). (Color online) O 1*s* and (b) Al 2*p* core level spectra from a decapped InGaAs sample and after subsequent *ex situ* NH_4OH treatment, 1 nm of Al deposition and 1 nm of ALD Al_2O_3. (c) Ratio of the fitted oxide to bulk peak components from the corresponding Ga $2p_{3/2}$, As $2p_{3/2}$, and In $3d_{5/2}$ spectra.

B. La deposition

Recently, lanthanum oxides have been explored as possible high-*k* materials on III–V surfaces due to the compatible chemistry as a group III element and its role in work function tuning.[37–43] In addition to these factors, La—as an extremely electropositive element—allows the discernment of chemical states such as As–Ga/As–Al bonds from that of As–La. Up to this point, there has been very little work on the effect of depositing La metal directly onto the (In)GaAs surface and as such there is virtually no information regarding the expected interactions between the La and the substrate. With that in mind the interaction of the La-IPL with an oxide-free InGaAs surface is shown in Fig. 8. Initial observations of the Ga and As $2p_{3/2}$ regions might indicate that the La-IPL behaves similarly to the Al-IPL; however, there are some significant differences. The deposition of La results in the formation of lower binding energy Ga and In peaks in their respective plots. The binding energy of these peaks is similar to that seen with the Al-IPL layer and, considering the significant difference in electronegativity between Al and La, this suggests that these peaks are due to metalliclike Ga–Ga and In–In bonding; however, some La bonding cannot be ruled out. In the case of the As peak, however, the emergence of a large lower binding energy peak, ~0.75 eV from the bulk peak, is clearly detected, indicating significant levels of As–La bonding taking place. This is in contrast to the Al-IPL case, where As–Al binding was at a very low level. There is also no evidence of As–As formation taking place.

If we contrast this to the case of $LaAlO_x$ deposition by ALD on the atomically clean $In_{0.2}Ga_{0.8}As$ case carried out by Aguirre-Tostado *et al.*,[43] where the La precursor was used as the first cycle in the deposition process and as such is a good allegory to the La metal deposition here, there is no evidence of Ga–Ga or In–In formation taking place in the Ga 2*p* and In 3*d* spectra. Also, for the As 2*p* spectra, there is no evidence of the large lower binding energy peak seen in this study, although As–As bond formation is detected due to disruption of the $In_{0.2}Ga_{0.8}As$ surface. This all highlights the significantly reduced interaction of the ALD La with the InGaAs substrate in comparison to direct metal deposition, due to the ligand interactions, which localize the La growth at the semiconductor surface.

Exposure to the ALD chamber at 300 °C causes gallium, indium, and arsenic oxidation, as well as emergence of large amounts of As–As bonding. This is concurrent with oxidation of the La layer, with the La 3*d* spectra in Fig. 9(a) having a peak position indicative of La_2O_3 or $La(OH)_3$. This is further confirmed by looking at the separation between the core level orbital peak and the peak due to the final state effect as a result of the bonding component of charge transfer from the ligand valence band to the core level (~4 eV), as well as the total spectral peak shape. This all suggests that the La–O is primarily in the form of $La(OH)_3$.[44] Determining the exact nature of the oxide layer from the O 1*s* layer in Fig. 9(b) is difficult due to the number of spectral components needed to accurately deconvolute the spectra, making accurate assignment more complex; however, the presence of components at the higher binding energy side of the spectra are again indicative of hydroxide formation.

After the anneal, metallic Ga or In is no longer detected, with the As–La state also greatly reduced. The Ga–O and In–O states formed as a result of exposure to the ALD reactor are not affected following TMA/water exposures, highlighted by the ratio of the oxide components to the corresponding substrate peaks in Fig. 9(c), suggesting that, again, these are located at the interface between the La–O and the substrate with the TMA unable to interact with it.

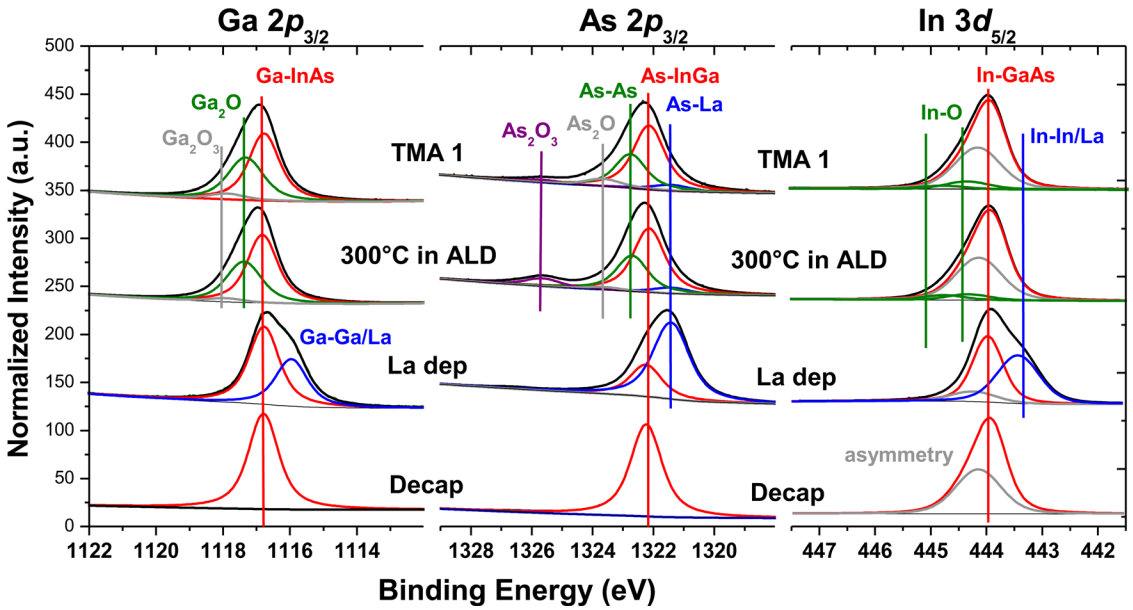

FIG. 8. (Color online) Ga $2p_{3/2}$, As $2p_{3/2}$, and In $3d_{5/2}$ core level spectra from a decapped InGaAs sample, after 1 nm of La metal deposition and first half-cycle of TMA.

Interestingly, the As^{3+} states are reduced by the subsequent TMA exposure, indicating that they may have formed on top of the La layer; however, it is also possible that arsenic oxides will reduce over time due to the elevated temperatures in the ALD reactor, potentially with oxygen transfer to gallium and indium,[23] or to the La layer.

From the Al 2*p* spectra in Fig. 9(d), it appears that with the first few cycles of TMA and water, based on the binding

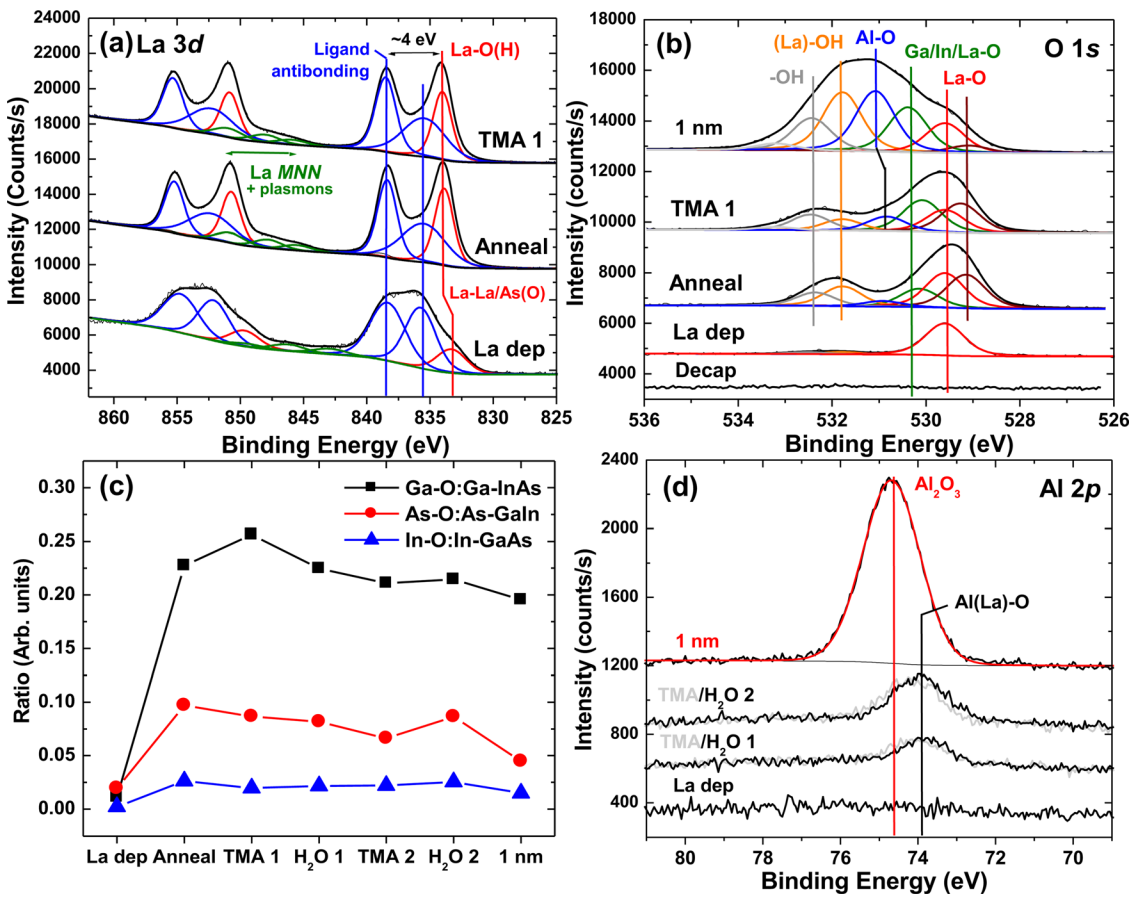

FIG. 9. (a) (Color online) La 3*d* core level spectra after La deposition on a decapped InGaAs sample, subsequent exposure to the ALD reactor at 300 °C, and first cycle of TMA. (b) Corresponding O 1*s* spectra, including the spectra after 1 nm of Al_2O_3 deposition. (c) Ratio of the fitted oxide components to the bulk peak from the Ga $2p_{3/2}$, As $2p_{3/2}$, and In $3d_{5/2}$ spectra. (d) Al 2*p* spectra.

energy position of the peak, there appears to be interaction between the La–O layer and the TMA. This manifests itself as a peak at a lower binding energy than would be expected for Al_2O_3, again consistent with La having a much lower electronegativity than Al. With subsequent cycles up to 1 nm of Al_2O_3 growth, we see the peak shift to a higher binding energy, suggesting more uniform Al_2O_3 formation; however, it is possible that Al–La–O bonding persists at the interface between the Al_2O_3 and the La-IPL.

IV. SUMMARY AND CONCLUSIONS

This study has revealed that on a pristine oxide-free surface, Al- and La-IPLs disrupt the system by breaking III–V bonds. In general, the ALD reactor environment oxidizes the metal layers and leads to Ga–O bond regrowth that cannot be controlled by subsequent TMA exposures. Some As–O regrowth is seen only with the La-IPL, as well as persisting As–La bonding, which is never fully removed. For both IPLs the final level of Ga–O present at the interface appears larger than following ALD directly on a clean surface, which could have significant consequences for the electrical performance for devices with Ga_2O_3 known to be a significant source of interface defects. Unlike TMA clean-up, the La/Al-IPLs generate reduction products in the form of metallic Ga and In states, which in the case of the Al-IPL are not removed upon oxidation of the Al. This observation supports earlier claims that reduction products of gallium oxides are volatilized during surface clean-up using TMA/water ALD reactions. It is concluded that the use of metallic IPLs may not be effective at generating high quality interfaces between high-*k* oxides and the oxide-free InGaAs surface due to the generation of metallic bonds at the III–V IPL interface and subsurface region. This metal interaction is mediated in the case of ALD deposition due to the interaction of the precursor ligands with the substrate ensuring a surface localized growth and preventing the formation of group III metallic states.

ACKNOWLEDGMENTS

This work was supported by the Semiconductor Research Corporation Focus Center Research Program Materials Structures and Devices Center, and the National Science Foundation under Electrical, Communications and Cyber Systems Award No. 0925844.

[1]*Fundamentals of III–V Semiconductor MOSFETs*, edited by S. Oktyabrsky and P.D. Ye (Springer, New York, 2010).
[2]C. L. Hinkle, B. Brennan, S. McDonnell, M. Milojevic, A. M. Sonnet, D. M. Zhernokletov, R. V. Galatage, E. M. Vogel, and R. M. Wallace, ECS Trans. **35**, 403 (2011).
[3]S. Oktyabrsky, V. Tokranov, M. Yakimov, R. Moore, S. Koveshnikov, W. Tsai, F. Zhu, and J. C. Lee, Mater. Sci. Eng., B **135**, 272 (2006).
[4]F. Zhu *et al.*, Appl. Phys. Lett. **94**, 013511 (2009).
[5]C. L. Hinkle, M. Milojevic, B. Brennan, A. M. Sonnet, F. S. Aguirre-Tostado, G. J. Hughes, E. M. Vogel, and R. M. Wallace, Appl. Phys. Lett. **94**, 162101 (2009).
[6]M. Milojevic, "Controlling interface chemistry of high mobility substrates through passivation layers and atomic layer deposition," Ph.D. dissertation (University of Texas at Dallas, 2010).
[7]M. Milojevic, C. L. Hinkle, F. S. Aguirre-Tostado, H. C. Kim, E. M. Vogel, J. Kim, and R. M. Wallace, Appl. Phys. Lett. **93**, 252905 (2008).
[8]C. L. Hinkle *et al.*, Appl. Phys. Lett. **92**, 071901 (2008).
[9]J. H. Yum *et al.*, J. Vac. Sci. Technol. A **29**, 061501 (2011).
[10]H. Iwakuro and T. Kuroda, Jpn. J. Appl. Phys., Part 1 **29**, 381 (1990).
[11]W. E. Spicer *et al.*, J. Vac. Sci. Technol. B **6**, 1245 (1988).
[12]C. B. Duke *et al.*, Phys. Rev. Lett. **46**, 440 (1981).
[13]D. Shoji, M. Shinohara, T. Miura, M. Niwano, and N. Miyamoto, J. Vac. Sci. Technol. A **17**, 363 (1999).
[14]S. P. Kowalczyk, J. R. Waldrop, and R. W. Grant, J. Vac. Sci. Technol. **19**, 611 (1981).
[15]A. Dimoulas, D. Tsoutsou, Y. Panayiotatos, A. Sotiropoulos, G. Mavrou, S. F. Galata, and E. Golias, Appl. Phys. Lett. **96**, 012902 (2010).
[16]S. D. Elliott, Surf. Coat. Technol. **201**, 9076 (2007).
[17]See: http://www.intelliepi.com.
[18]B. Shin, J. B. Clemens, M. A. Kelly, A. C. Kummel, and P. C. McIntyre, Appl. Phys. Lett. **96**, 252907 (2010).
[19]Picosun Oy.: http://www.picosun.com.
[20]P. Sivasubramani, J. Kim, M. J. Kim, B. E. Gnade, and R. M. Wallace, J. Appl. Phys. **101**, 114108 (2007).
[21]R. M. Wallace, ECS Trans. **16**, 255 (2008).
[22]A. Herrera-Gómez, P. Pianetta, D. Marshall, E. Nelson, and W.E. Spicer, Phys. Rev. B **61**, 12988 (2000). AANALYZER is software for XPS peak deconvolution and is available from http://qro.cinvestav.mx/~aanalyzer/AANALYZER.
[23]B. Brennan and G. Hughes, J. Appl. Phys. **108**, 053516 (2010).
[24]B. Brennan, M. Milojevic, C. L. Hinkle, F. S. Aguirre-Tostado, G. Hughes, and R. M. Wallace, Appl. Surf. Sci. **257**, 4082 (2011).
[25]C. L. Hinkle, M. Milojevic, E. M. Vogel, and R. M. Wallace, Appl. Phys. Lett. **95**, 151905 (2009).
[26]G. P. Schwartz, Thin Solid Films **103**, 3 (1983).
[27]M. L. Huang, Y. C. Chang, C. H. Chang, Y. J. Lee, P. Chang, J. Kwo, T. B. Wu, and M. Hong, Appl. Phys. Lett. **87**, 252104 (2005).
[28]W. Wang, C. L. Hinkle, E. M. Vogel, K. Cho, and R. M. Wallace, Microelectron. Eng. **88**, 1061 (2011).
[29]H.-P. Komsa and A. Pasquarello, Microelectron. Eng. **88**, 1436 (2011).
[30]J. Robertson, Appl. Phys. Lett. **94**, 152104 (2009).
[31]See: http://www.webelements.com/electronegativity.html.
[32]A. J. Bard, R. Parsons, and J. Jordan, *Standard Potentials in Aqueous Solution, International Union of Pure and Applied Chemistry* (Dekker, New York, 1985).
[33]M. V. Lebedev, D. Ensling, R. Hunger, T. Mayer, and W. Jaegermann, Appl. Surf. Sci. **229**, 226 (2004).
[34]R. L. Puurunen, Appl. Surf. Sci. **245**, 6 (2005).
[35]B. Brennan, M. Milojevic, H. C. Kim, P. K. Hurley, J. Kim, G. Hughes, and R. M. Wallace, Electrochem. Solid-State Lett. **12**, H205 (2009).
[36]P. D. Ye *et al.*, Appl. Phys. Lett. **83**, 180 (2003).
[37]D. Choi, J. S. Harris, M. Warusawithana, and D. G. Schlom, Appl. Phys. Lett. **90**, 243505 (2007).
[38]Y. Liu, M. Xu, J. Heo, P. D. Ye, and R. G. Gordon, Appl. Phys. Lett. **97**, 162910 (2010).
[39]H. Zhao, J. H. Yum, Y.-T. Chen, and J. C. Lee, J. Vac. Sci. Technol. B **27**, 2024 (2009).
[40]W. Chia-Song and L. Hsing-Chung, J. Semicond. **30**, 114004 (2009).
[41]M. I. Medina-Montes, M. V. Selvidge, A. Herrera-Gomez, F. S. Aguirre-Tostado, M. A. Quevedo-Lopez, and R. M. Wallace, J. Appl. Phys. **106**, 053506 (2009).
[42]D. Fuks, S. Dorfman, J. Felsteiner, L. Bakaleinikov, A. Gordon, and E. A. Kotomin, Solid State Ionics **173**, 107 (2004).
[43]F. S. Aguirre-Tostado, M. Milojevic, B. Lee, J. Kim, and R. M. Wallace, Appl. Phys. Lett. **93**, 172907 (2008).
[44]M. F. Sunding, K. Hadidi, S. Diplas, O. M. Løvvik, T. E. Norby, and A. E. Gunnæs, J. Electron. Spectrosc. Relat. Phenom. **184**, 399 (2011).